Bachelor Project

**Czech
Technical
University
in Prague**

F3
Faculty of Electrical Engineering

Design of Robot for Carbon Fiber Laying

Tereza Uhrová

Supervisor: Ing. Vladimír Smutný, Ph.D.
Field of study: Cybernetics and Robotics
May 2021

ZADÁNÍ BAKALÁŘSKÉ PRÁCE

I. OSOBNÍ A STUDIJNÍ ÚDAJE

Příjmení: **Uhrová**   Jméno: **Tereza**   Osobní číslo: **483546**

Fakulta/ústav: **Fakulta elektrotechnická**

Zadávající katedra/ústav: **Katedra kybernetiky**

Studijní program: **Kybernetika a robotika**

II. ÚDAJE K BAKALÁŘSKÉ PRÁCI

Název bakalářské práce:

Návrh průmyslového robotu pro kladení uhlíkového vlákna

Název bakalářské práce anglicky:

Design of Robot for Carbon Fiber Laying

Pokyny pro vypracování:

Seznam doporučené literatury:

[1] Robotic Operating Systém, https://www.ros.org/
[2] X Winder, https://xwinder.com/
[3] Tugay Üstün et al.: Evaluating the Effectiveness of Nanofillers in Filament Wound Carbon/Epoxy Multiscale Composite Pipes, April 2016, Composites Part B Engineering 96 DOI: 10.1016/j.compositesb.2016.04.031
[4] Saad A. Mutasher et al.: Small-scale filament winding machine for producing fiber composite products, April 2012Journal of Engineering Science and Technology 7(2):156-168

Jméno a pracoviště vedoucí(ho) bakalářské práce:

Ing. Vladimír Smutný, Ph.D.,   robotické vnímání   CIIRC

Jméno a pracoviště druhé(ho) vedoucí(ho) nebo konzultanta(ky) bakalářské práce:

Datum zadání bakalářské práce: **03.12.2020**   Termín odevzdání bakalářské práce: **21.05.2021**

Platnost zadání bakalářské práce: **30.09.2022**

_____   _____   _____
Ing. Vladimír Smutný, Ph.D.   prof. Ing. Tomáš Svoboda, Ph.D.   prof. Mgr. Petr Páta, Ph.D.
podpis vedoucí(ho) práce   podpis vedoucí(ho) ústavu/katedry   podpis děkana(ky)

III. PŘEVZETÍ ZADÁNÍ

Studentka bere na vědomí, že je povinna vypracovat bakalářskou práci samostatně, bez cizí pomoci, s výjimkou poskytnutých konzultací. Seznam použité literatury, jiných pramenů a jmen konzultantů je třeba uvést v bakalářské práci.

_____   _____
Datum převzetí zadání   Podpis studentky

Acknowledgements

I would like to thank my supervisor Ing. Vladimír Smutný, Ph.D. for his advice and guidance. I am very grateful to my family for all the support and warm meals.

Declaration

I declare that this thesis has been composed solely by myself and that it has not been submitted, in whole or in part, in any previous application for a degree. Except where stated otherwise by reference or acknowledgment, the work presented is entirely my own. I have followed the rules set by the Code of Ethics for Students and Researchers.

Prague, 21. May 2021

Abstract

Composite material applications have been rapidly developing in the recent decades. Our robot is based on a standard filament winding machine and has been upgraded with a planar manipulator with three degrees of freedom.

We have tested and selected a sensor for detecting obstacles during fiber laying. We optimized robot arm's dimension, created a virtual model of our automated system in ROS and wrote trajectory planning software. The planner computes collision-free trajectory of fiber laying for a complex product based on its parameters.

Keywords: composite materials, carbon fiber laying, trajectory planning, computer-integrated manufacturing

Supervisor: Ing. Vladimír Smutný, Ph.D.
CIIRC CTU

Abstrakt

Využití kompozitních materiálů se v posledních dekádách rychle rozšiřuje. Náš robot je založen na standardním navíjecím stroji a byl rozšířen o planární manipulátor se třemi stupni volnosti.

Otestovali a vybrali jsme senzor na detekci překážek v průběhu kladení vlákna. Optimalizovali jsme rozměry robotické ruky. Vytvořili jsme virtuální model našeho automatického systému v ROS a napsali jsme program na plánování trajektorie. Tento plánovač spočítá bezkolizní trajektorii kladení vlákna pro komplexní výrobek podle jeho parametrů.

Klíčová slova: kompozitní materiály, kladení uhlíkového vlákna, plánování trajektorie, počítačem řízená výroba

Překlad názvu: Návrh průmyslového robotu pro kladení uhlíkového vlákna

Contents

Chapter **1**

Introduction

In recent years, automation and robotics have been rapidly developing in industrial applications. An automated machine or a robot can do all the heavy work without needing breaks, and it is also not threatened by the current pandemic or shortage of personnel. Robots are not endangered as easily as human employees when working, for example, with toxic chemicals.

Composite material applications in industry, transport, aerospace, etc. rapidly advanced in the past decades, carbon fiber composites are lighter and stronger than, for example, aluminum or steel parts, and thus there has been a significant increase in their applications.

CompoTech [1] is a company that focuses on engineering and producing high-performance composite material products. They design their products and technologies specifically for a customer's requirements. They also develop their own production technology (including machinery and software). CompoTech invests in automation and robotics. The company based their technology on a standard filament winding.

In this thesis, we design a robot for carbon fiber laying to automate production of a complex product that CompoTech developed. The base of this robotic system is an existing machine that lacks in performance and human assistance is needed at all times. We will replace part of this machine with a planar robotic arm with a sensor, so the system can work without supervision.

Chapter 2

Motivation

Standard filament winding technology (Fig. 2.1) involves winding filaments under tension over a rotating mandrel. The mandrel rotates around the spindle while a delivery nozzle on a carriage traverses horizontally in parallel with the axis of the rotating mandrel, laying down fibers in the desired pattern. The most common filaments are made from glass or carbon and are impregnated with resin by passing through a bath during the winding. Once the winding is finished, the resin is cured. Then the mandrel is removed, leaving the hollow final product[2].
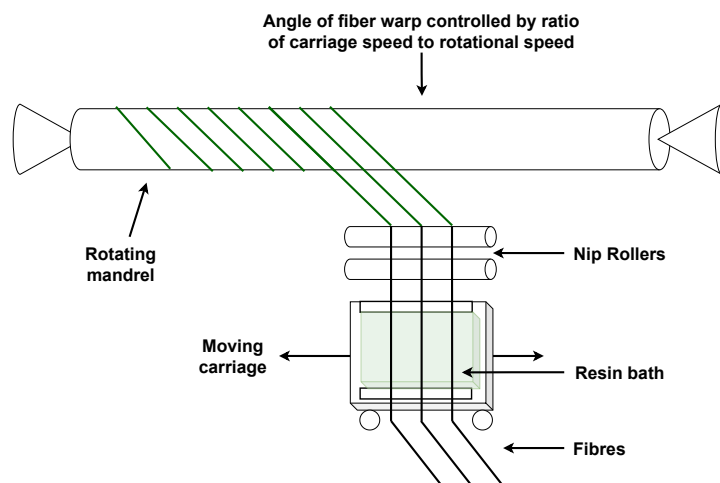
Figure 2.1: Schematic of standard filament winding technology

In the beginning, CompoTech innovated standard old filament winding technology by implementing pins (Fig. 2.2) at the end of a mandrel [2] to enable the production of tubes or beams with axial fibers [3] (parallel to rotational axis). Carbon epoxy beam produced with parallel fibers in tension has 10 to 15% higher stiffness in the axial direction and up to 50% greater bending strength compared to using conventional filament winding techniques.
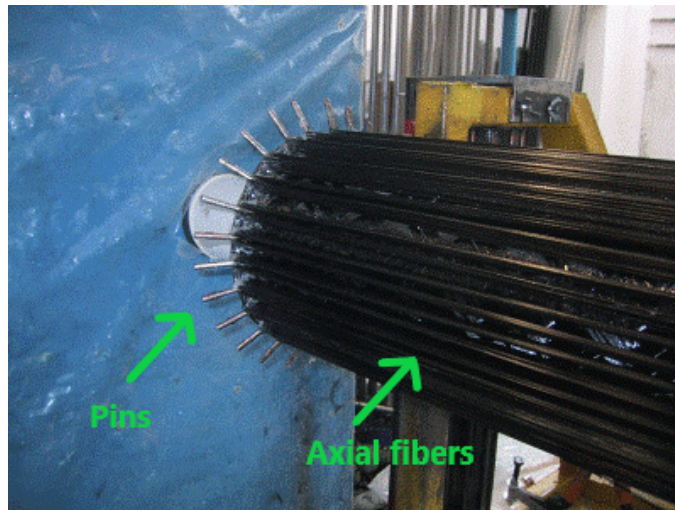
Figure 2.2: Pins (thin wires on the end of the mandrel) on the end of the mandrel enable to wind the axial fibers (fibers wound in parallel to the mandrel)

Today, the trend is to produce parts with added functions like integrated loop technology [4] (further ILT, see example Figure 2.3). The incorporation of a mechanical fixing and fastener system, which can be sometimes molded in, is often a secondary manufacturing step. That adds production time and cost. Composite parts then need fixture holes drilled through the fiber-reinforced polymer (FRP) laminate where bonding is insufficient. The dilemma for many designers is the fact that the drilling of fixture holes cuts through reinforcement fibers and reduces the mechanical properties of the laminate. To overcome this loss of performance, FRP mold designs are prepared for additional layers of reinforcement at load bearing fixing point areas to be built in the composite part during production. However, the downsides are that the components become even heavier, and further material cost is added.

Figure 2.3: Tubes with ILT [1]

CompoTech has developed a continuous axial fiber integrated loop technology (ILT) process which can overcome joint design issues. It offers manufacturers an automated system for rapid and cost-effective production of lighter and stronger FRP epoxy composite tubular structural parts with fully integrated joints between sub-assembly components.

Key ILT production and performance benefits include:

- Efficient material use

- Reduced machining

- Reduced overall production and labor time

- Stronger joints

Integrated loop joints are typically formed around a metal tooling mandrel. Inserts, such as a metal sleeve, can also be incorporated inside the looped joint section during production. Continuous wet epoxy resin impregnated carbon fibers are accurately placed and wound in orientations to provide the required stiffness, compression, flexural and torsional forces needed. Once individual components have been fully cured, they are ready to be assembled. The advantage of ILT parts is that fewer assembly parts and production operations are needed. Sub-assembly components can be positioned and rapidly bonded together by applying suitable two-part epoxy structural adhesive to the integrated loop contact area. The final bonded ILT joint provides superior performance.

ILT technology requires a more complex fiber laying path than traditional filament winding. This is possible to achieve very effectively with a specifically designed robot arm, which is the main motivation of this bachelor thesis.

Chapter **3**

Automation of Carbon Fiber Composites Manufacturing

One of the main advantages apart from the physical properties of composite materials is the possibility to automate their production process. However, the application of robotic automation in mass production of high-performance composites is not new. A great example is the success of Boeing 787 Dreamliner [5], the first aircraft which hull body is all carbon fiber composite (Figure 3.1). Due to the production of Dreamliner's hull is automated, Boeing can produce the plane faster and more effectively. The competition (Airbus) was producing their aluminum hull bodies mostly manually. As a result, Boeing could take a higher stake of aircraft orders and lead the market (approximately 10 to 15 years ago).
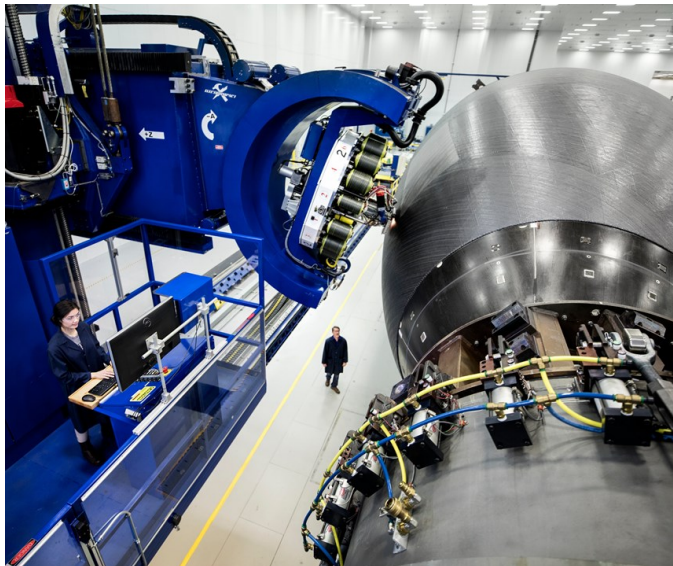
Figure 3.1: Production of Boeing fuselage structure [5]. The blue robot is carrying bobbins and winding it on a curved structure

Most carbon fiber composite producers of aerospace applications are using pre-impregnated fibers with epoxy resin, so-called prepregs, which were developed in 70ths in the last century. The level of chemistry, in those years,

could not produce a resin with sufficient strength and toughness processable in a room temperature. Prepregs are still used in current plane production due to the relative conservatism of the aerospace industry. Prepreg at room temperature is very tacky. This is the main principle of automated laying heads.

Figure 3.2: Prepreg tape laying head on a robot arm (white structure) [6]

Laying heads can start anywhere in the mold/mandrel/tool simply by pressing the beginning of pre-impregnated fiber. They can place the required pattern of layers and cut the fiber at any position. Infrared or laser beam can also be used to heat prepreg locally and increase tackiness during the laying process. After laying pre-impregnated carbon fibers, the product needs to be hardened in an autoclave (a pressure vessel with controlled temperature/pressure, see Figure 3.3).

Figure 3.3: Autoclave example [7]

The autoclave process still requires lots of manual work (e. g. manipulation with molds, tools) and consumable materials as vacuum bags and vacuum layers. Even though the carbon fiber is deposited automatically, the overall process cost is quite high.

Prepreg laying heads usually work with prepreg tape or prepreg tow. Prepreg tow is produced by pre-impregnating fiber tow directly from fiber bobbin (Figure 3.4).

Figure 3.4: Example of fiber towpreg bobbin[8]

Another principle of a typical laying head is that the towpreg bobbin is carried with the head. Heads, which can be used with standard industrial robots, can usually carry a very limited number of towpreg bobbins due to the limited payload of industrial robots. For example, the laying head from Mikrosam [9] has, according to Figure 3.5, only 4 bobbins of towpreg and is using one of the largest sizes of Kuka robot. The estimated weight of such a laying head can be about several hundreds of kilograms.
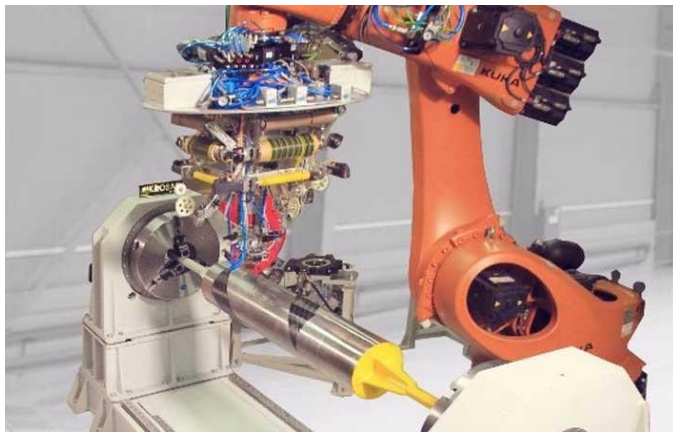
Figure 3.5: Towpreg laying head from Mikrosam[9] carried by a robot arm (orange)

To deposit a larger number of towpreg for larger aerospace structures like aircraft hull or wing laying heads need to carry tens of bobbins. Then the special multi-axis manipulators have to be built (See Figure 3.6). These manipulators are usually using gantry structures, which is why these automatic systems are often build by companies with experience in large 6 axis milling machines, for example, Fives Cincinnati, Ingersoll Machine Tools [10].

Figure 3.6: Ingersoll Mongoose fiber laying system [11]

Due to the complexity and the costs connected with prepreg composite manufacturing as described above, the modern trends are "out of autoclave" technologies (so-called OOA [12]). These trends are also enabled by advancements in epoxy resin chemistry and especially nanoparticles. There is new demand to automate production processes using wet impregnated fibers.

There are not many companies developing a solution to automate laying process using wet impregnated fibers yet. One example could be MF Tech [13] which is using the Kuka robot to improve standard wet filament winding technology (Figure 3.7), but the Kuka robot arm is only a replacement for gantry type machine, maybe the added value is in special manipulation features.

Figure 3.7: MF Tech system for standard filament winding [13]

CompoTech has also developed an automated wet impregnated carbon fiber laying process called RAFL (Robot-assisted fiber laying). RAFL use Fanuc 35kg payload robot on machine x-axis carriage to lay up to 8 wet impregnated fibers with high precision and quality using pressing rollers. RAFL system is also able to lay more complex shapes and patterns in high

deposition rate (i.e. how fast is the fiber layered). CompoTech's motivation to use continuous wet impregnation is also better thermal and dimensional stability than prepreg which tends to drift in dimension due to residual stress from the curing process in an autoclave. Hence why prepreg parts are not suitable for applications in mechanical engineering or machine building.

Figure 3.8: CompoTech RAFL (Robot assisted fiber laying) system where FANUC robot arm (upper yellow part) is laying carbon fiber on to the mandrel(black tube under the robot arm)

The ILT, as described above in Chapter 1, was developed by CompoTech on modified X-winder, filament winding machine with 4 driven axis.

Further modifications of this CompoTech developing machine with a specifically built robot arm shall increase its capability and prove the concept of mass ILT production using industrial robots.

**Figure 3.9:** 4 axis filament winding machine X-winder [14]

3.1 X-winder structure

X-winder is a tabletop filament winding machine with 4 driven axes. After CompoTech purchased it, the machine was further modified to suit the company's needs (Figure 3.10). The machine is now controlled with MACH3, a control system for CNC machines.
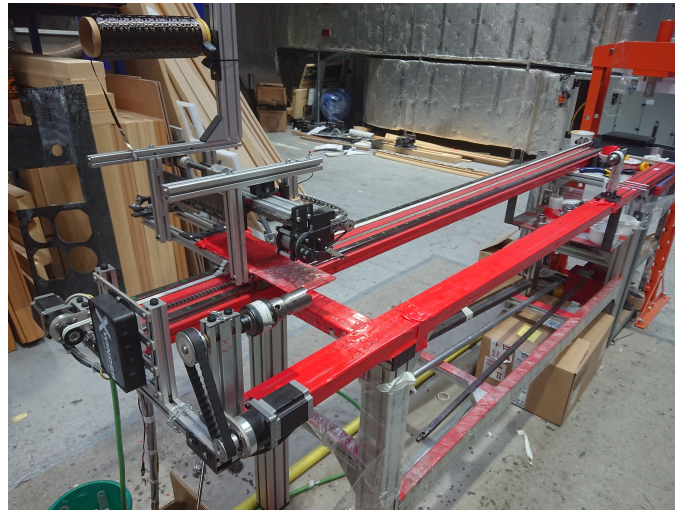
Figure 3.10: Modified X-winder (the red machine)

The joints are shown in figure 3.11. The red axis is a mandrel rotation. Purple axis is the translation of a carriage along the mandrel, which has a range of motion 0 to 2600 millimeters. The green axis is translation of endpoint perpendicular to the mandrel with a maximum of 230 millimeters, that reaches several centimeters beyond the mandrel axes. The blue axis represents the rotation of the endpoint nozzle. All the aforementioned axes are driven by stepper motors.
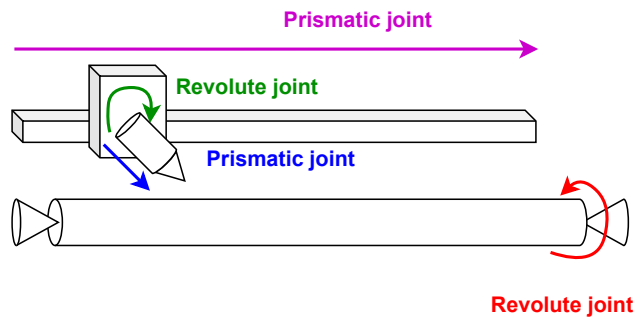

Figure 3.11: Scheme of X-winder and its joints

The task of this thesis is to replace X-winder's blue and green axes with planar robot arm, which has three degrees of freedom.

13

Chapter 4

Detection of real positions of pins

CompoTech's winding technology with pins causes further problems. The resin impregnated carbon fibers run through the nozzle and are laid on the mandrel. The nozzle needs to guide and place the fiber between the pins (Figure 4.1). The fiber should be hooked from behind the pins. When the pins are used repeatedly and bent, the nozzle can collide with the pins. By implementing a sensor to the robot arm to measure actual positions of the pins, the possible collision of the nozzle carrying carbon fiber with the pins is prevented.
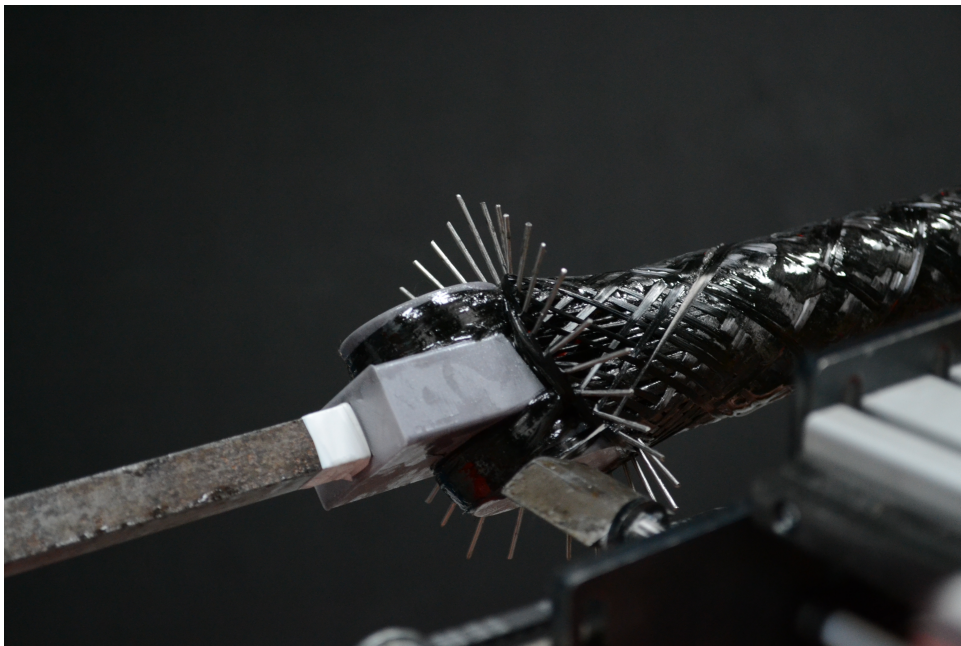
Figure 4.1: The nozzle is going through pins

Furthermore, we also considered when and how the pin detection should take place. Pins' positions can be measured during the fiber laying process, or they can be scanned before the manufacturing begins. In the first case, the nozzle already carries impregnated fiber, and sudden changes to a trajectory can alter the final pattern and slow down the laying process.

In the second case, the robot arm would scan pins at the ends of assembled mandrel without any carbon fiber or resin, saved positions of the pins and trajectory planning software would generate collision-free trajectory. We have decided to proceed with this option.

CompoTech lent us pin samples to test the sensors (Figure 4.2). Pins, a set of wires, are attached to a steel component, a pin holder that fits at the end of the mandrel. The samples varied in number and size of pins, as well as how long they have been used in production. The thinnest pins have a diameter of 1 mm.

Figure 4.2: New and shiny pin holder (left), slightly used pin holder (middle), heavily used pin holder (right)

To simulate the pin detection process, we have used a turntable mounted on an aluminum structure (Figure 4.3) to mimic the use of the sensor during carbon fiber laying. The pin holder is mounted on the rotating table with a simple 3D printed piece, with the sensor attached on the end of the arm.
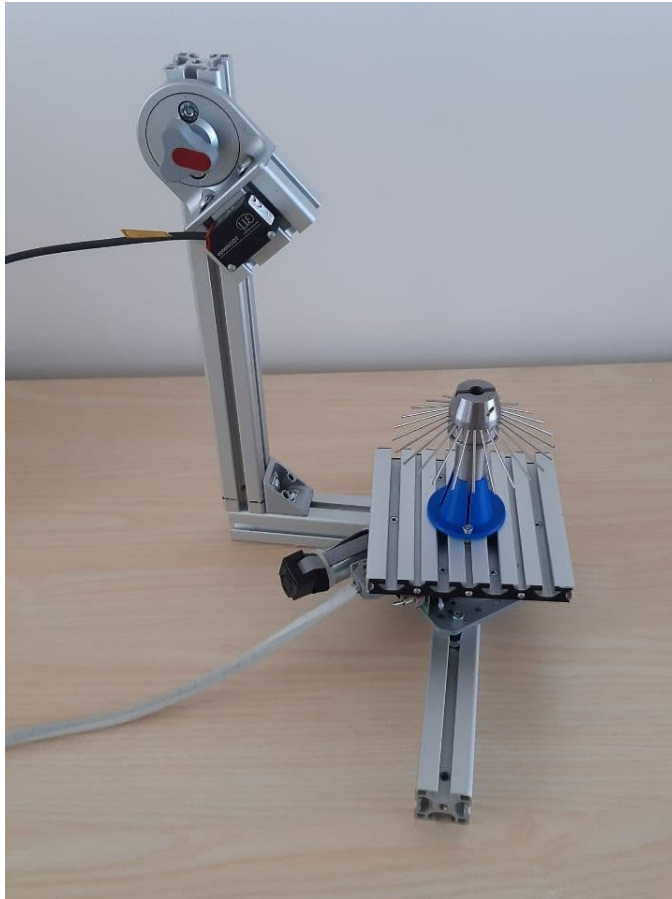
Figure 4.3: Sensor (black box on top) testing system with turn table, the pin holder is held by blue plastic piece

▉ 4.1   Photoelectric sensor SICK WTT12LC-B2533

There is a company that has been working on a pin detection system already. We borrowed a sensor SICK WTT12LC-B2533 from their system to test it.

Photoelectric sensor SICK works on the time-of-flight principle, and its communication interface is IO-Link V1.1. IO-Link is an industrial communication protocol. The sensor was connected to ifm AL1100 IO-Link master with Profinet interface. Profinet is another industrial communication protocol. We would need to get a different communication convertor to even be able to connect sensor SICK WTT12LC-B2533 to the computer since CompoTech does not use any of these industrial communication protocols.

We have decided not to use this sensor because of high cost and the complexity of the final system.

■ 4.2 Laser triangulation displacement sensor Micro-epsilon optoNCDT ILD1420-200

Additionally, we borrowed a sensor optoNCDT ILD1420-200 from Micro-Epsilon [15] for experiments. Laser triangulation displacement sensor optoN-CDT has a much more accessible interface RS422 which we used. This sensor has a measuring range 200 mm, starting from 60 mm.

In Matlab, we made an interface that configures the sensor, receives and decodes the output data. The outputs are distance, intensity, shutter and time stamp. These values are shown in graphs in relation to table rotation. There is one line for one table revolution. We measured ten rotations of the table.

In figure 4.4, we can see graphs corresponding to new pin holder, which is shiny and pins are evenly spaced. The indents in the graphs represent positions of each pin in relation to the pin holder rotation. Shutter is duration of the measurement. We can also observe intensity of laser beam.
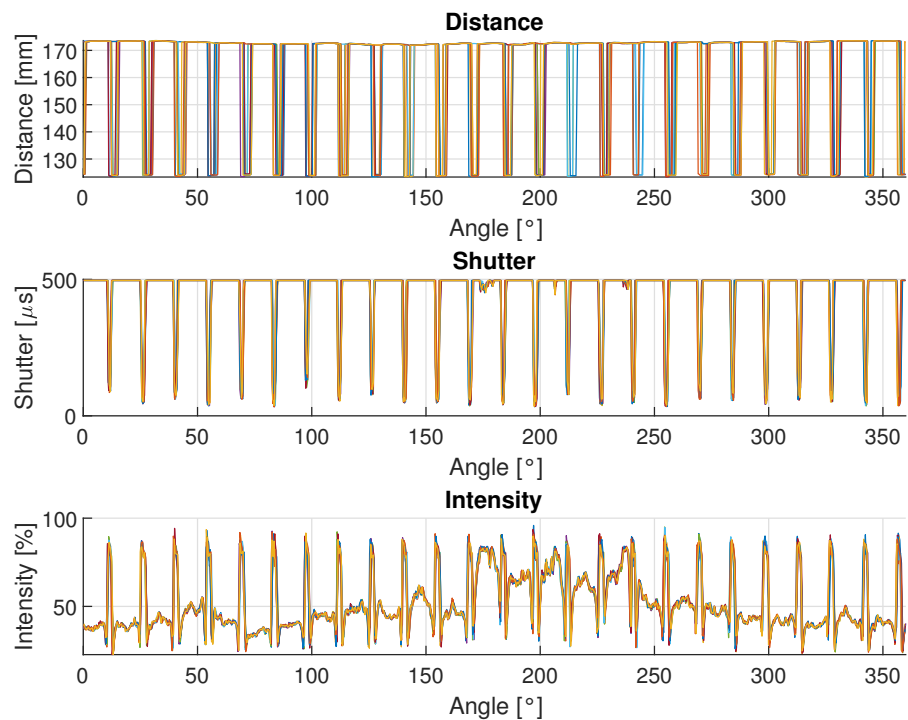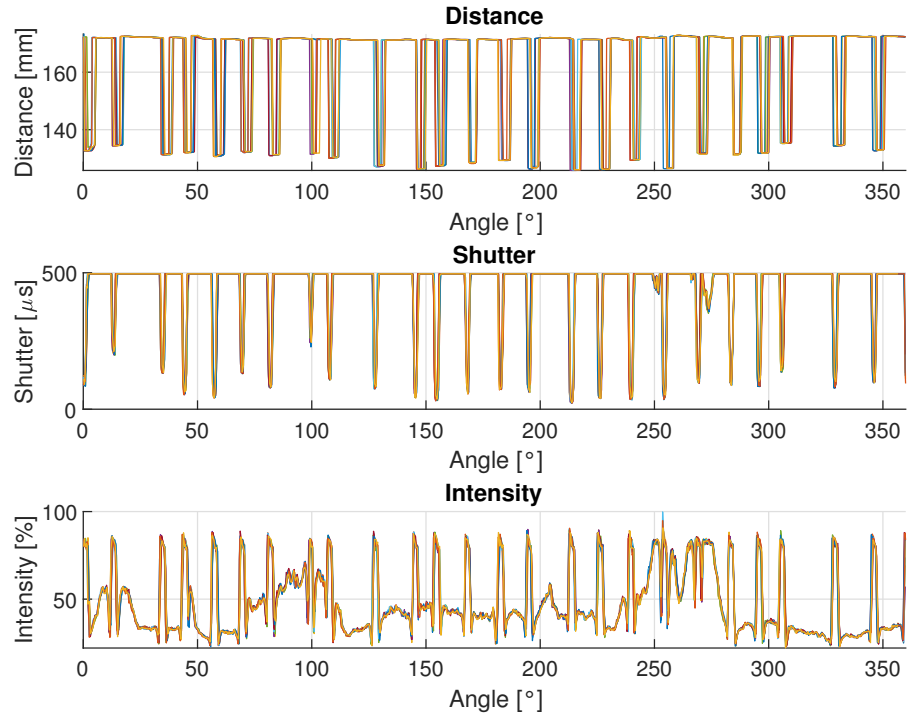

Figure 4.4: optoNCDT ILD1420-200 output data for new pin holder

18

In figure 4.5, we can see graphs corresponding to slightly used pins. There are visible irregularities in distance and shutter.
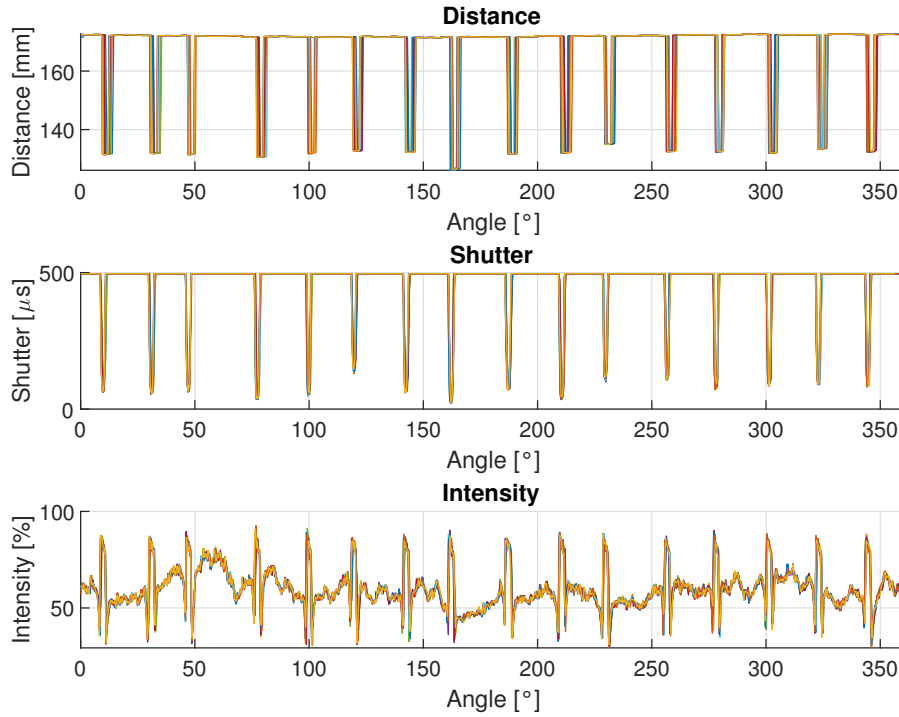
Figure 4.5: optoNCDT ILD1420-200 output data for slightly used pin holder

19

In Figure 4.6, we can see graphs corresponding to the heavily used pin holder. It is covered by old resin, and the pins are bent in various directions. There are visible irregularities in distance, shutter and intensity.

Figure 4.6: optoNCDT ILD1420-200 output data for heavily used pin holder

In total, we measured six different pin holders. Two of them were new with 25 thin (1 mm diameter) pins, two of them were used with 5 thicker (5 mm diameter) pins, one was heavily used with 25 thin pins and one was slightly used with 16 thin pins.

When we took a closer look on the measured distance, we noticed that the sensor did not capture a thin pin in some cases. In Figure 4.7, we can see that during one revolution (represented by the light blue line) the sensor did not register a change of the distance, which means a pin was skipped. Nevertheless, if we look at the same revolution (light blue line) in shutter and intensity, we can see that the sensor reacted as if the pin was captured. We decided to use shutter data for measuring of positions of thin pins.
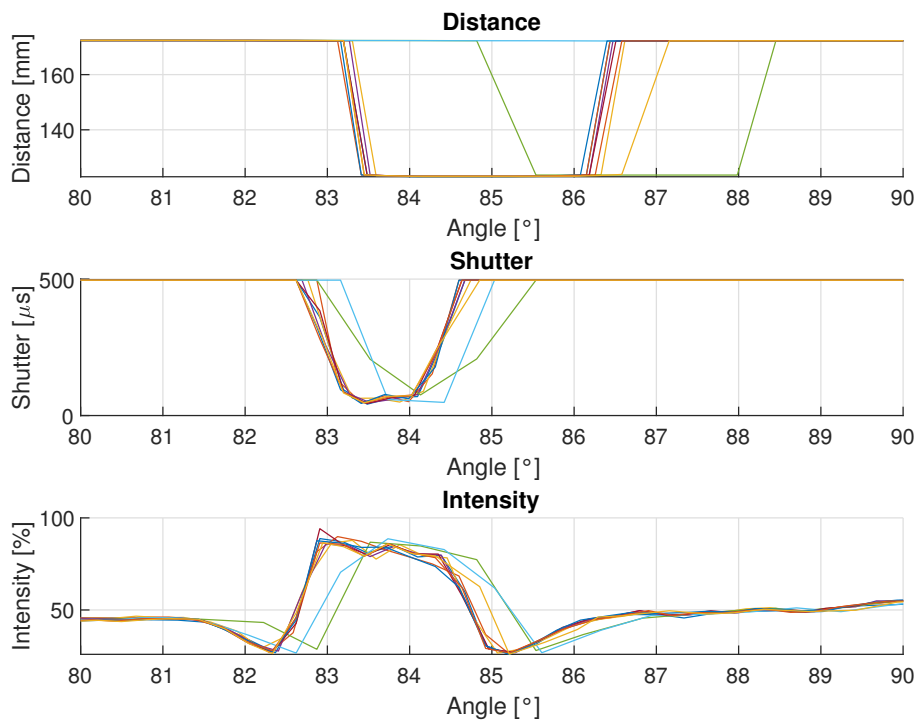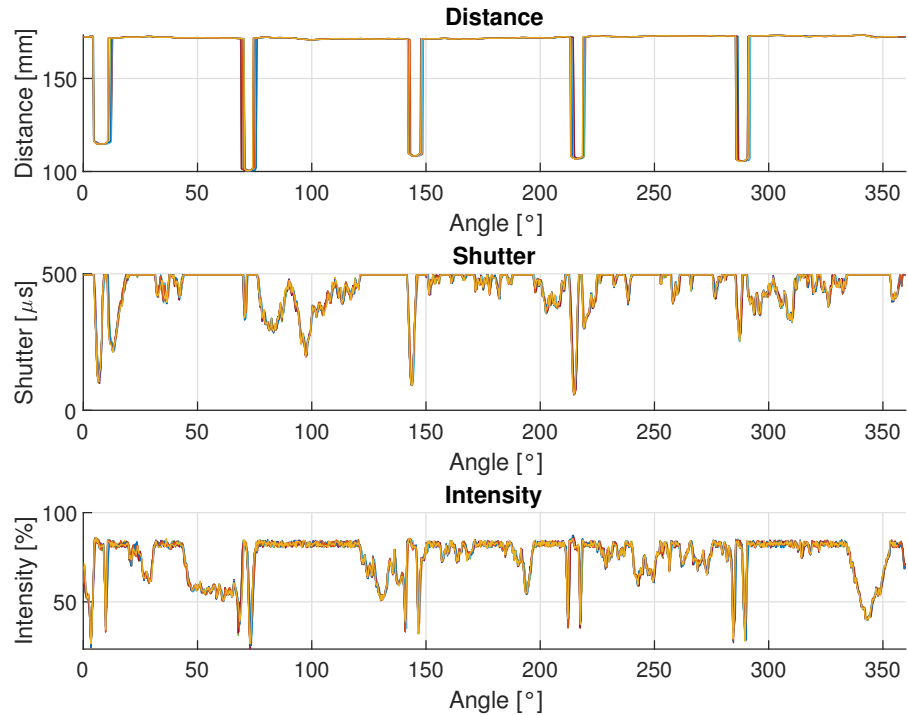

Figure 4.7: Detail of optoNCDT ILD1420-200 output data for new pin holder. The light blue line represents an error in distance, but not in shutter and intensity.

We wrote an evaluation script in Matlab. If the shutter is shorter than the threshold, a pin is detected. If the shutter is longer than the threshold, there is no pin. The script then makes an average from the angle where it starts detecting a pin, and from the angle where it stops detecting a pin. Each pin is now represented by its angular position.

The program calculates standard deviation for each pin in a pin holder, and then it computes an average standard deviation for all pins in the pin holder. These values are in following table:

Pin holder	Average standard deviation [°]
New 1	0.2392
New 2	0.2481
Slightly used	0.2119
Heavily used	0.2920

When we examined data for thick pins (Fig. 4.8), we looked at shutter and realized that the evaluation method for thin pins would not work for thick pins. The shutter does not have clear changes for pins, but in this case, the pins are thicker and there were no missed pins in distance data.

Figure 4.8: optoNCDT ILD1420-200 output data for the pin holder with thick pins

We altered the evaluation script. The pin's angular position is computed from distance data the same way as before. The average standard deviations for pin holders with thick pins are in the following table:

Pin holder	Average standard deviation [°]
Thick pins 1	0.4276
Thick pins 2	0.4514

The average standard deviations for all pin holders are sufficiently small. We were not able to research why the sensor miss a thin pin in distance data, but not in shutter and intensity. The problems in detection were found when the sensor was already returned to distributor.

Chapter 5

Optimization of robot arm's dimension

The robot arm will have three rotational joints and it will be mounted on X-winder's carriage, that moves along the mandrel, as shown in figure 5.1. The arm has three links. The first two have the same length and the third is the shorter endpoint link.
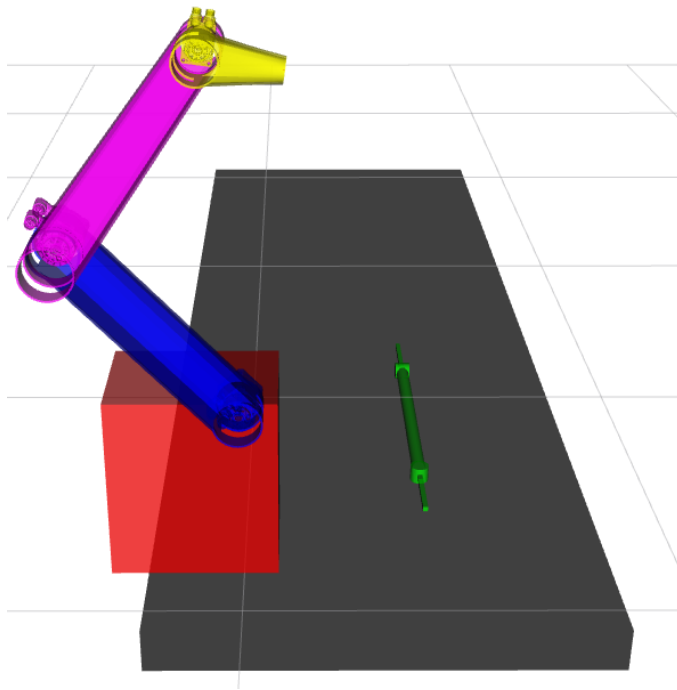
Figure 5.1: Simulation of X-winder with the robot arm

Dimensions of the arm need to be chosen carefully, so the endpoint nozzle reaches around the mandrel as shown in figure 5.2. The minimal requirement is that the nozzle reaches 180 degrees around the mandrel. This is represented by the green lines in the picture. The optimal requirement is that the nozzle reaches 220 degrees around the mandrel. That is represented by the red lines.
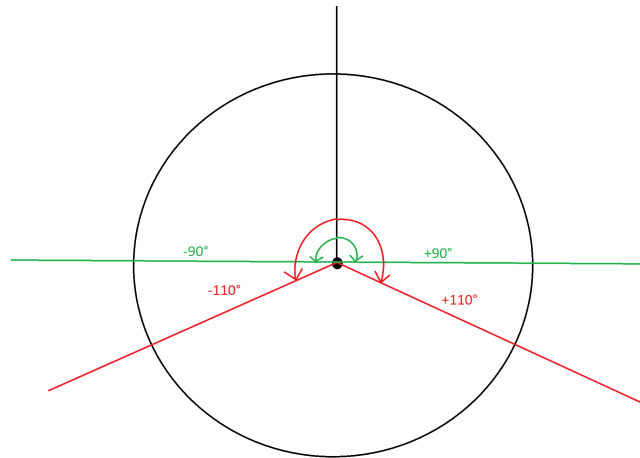
**Figure 5.2:** Cross section of mandrel with required working space

The Robot Operating System (ROS)[16] is a set of software libraries and tools for robot design and control. We have created a simplified but accurate model of the X-winder with the robot arm and visualized it in RViz, ROS visualization widget.

This simulation checks if the whole machine in a given state is not colliding with any objects. Dimensions of the robot arm and the place where it is mounted on the X-winder can be easily altered in this simulation.

MoveIt[17] is a motion planning software bundle for robotics that is used with ROS. Thanks to MoveIt, we were able to simulate X-winder's movement. At first, we have written a script that checks positions around the mandrel. The robot will try to move into 10 positions around the mandrel with the minimum diameter, and then it will try to do the same with a maximum diameter mandrel.

However, this is not the way to optimize robot arm dimensions. When we want to change the dimensions, we need to edit the robot model manually. So we have written a python script that checks collisions only with arm and mandrel, and computes it for a combination of different link lengths. The arm is simplified to three rectangles, and the mandrel is a circle, as seen in figure 5.4.
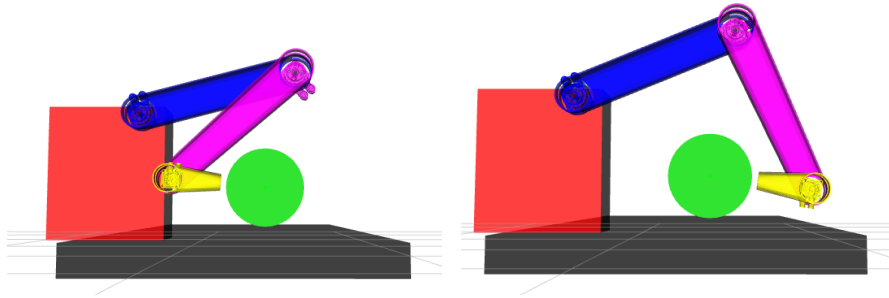
Figure 5.3: Example of simulation
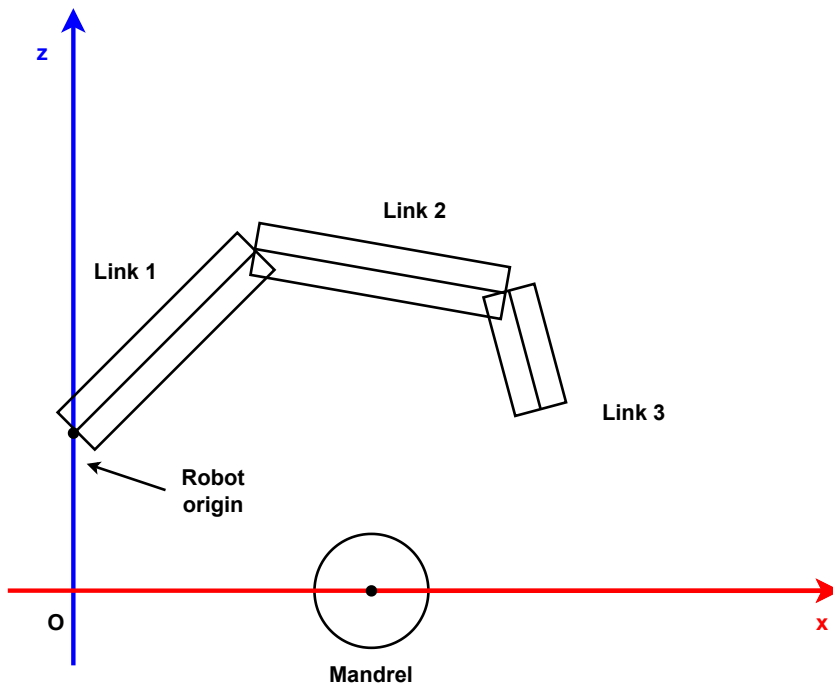
Figure 5.4: Visualization of simplified collision checker for optimizing robot dimensions

This collision checker then computes inverse kinematics and checks if the position is possible for 360 points around the mandrel for every dimension combination without collisions. The output is how many positions are achievable consecutively for given dimensions of the robot arm and mandrel.

Inputs for the checker are length intervals for all links, coordinates of robot arm origin and mandrel diameter. The checker then searches through the link lengths with a given step.

At first, we chose big intervals (200 mm to 700 mm for the second and first link, 100 mm to 350 mm for the third link) and 50 mm step. The contour graph of this test can be seen in figure 5.5. It is clear that the robot does not satisfy even minimal requirements for working space for short lengths of robot links, but as the length of the first and second link grows, the angle around the mandrel increases. When the dimensions are too big, the speed of growth of the angle around the mandrel decreases.
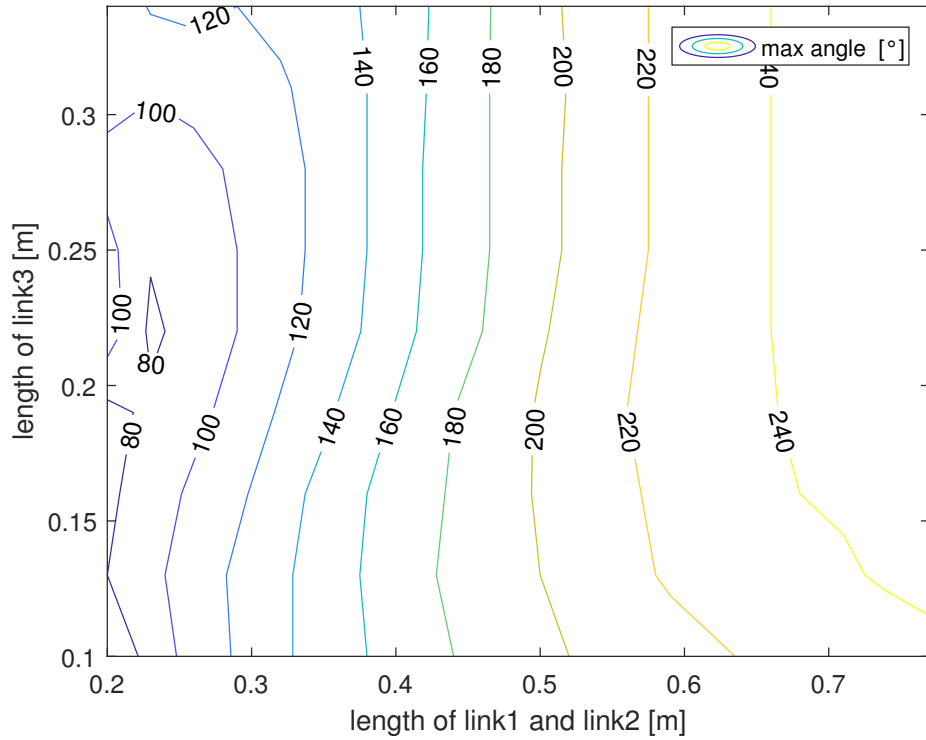
Figure 5.5: Optimization results for a wide range of input link lengths

The next test focused on smaller intervals with 10 or 20 mm step (Figure 5.6).
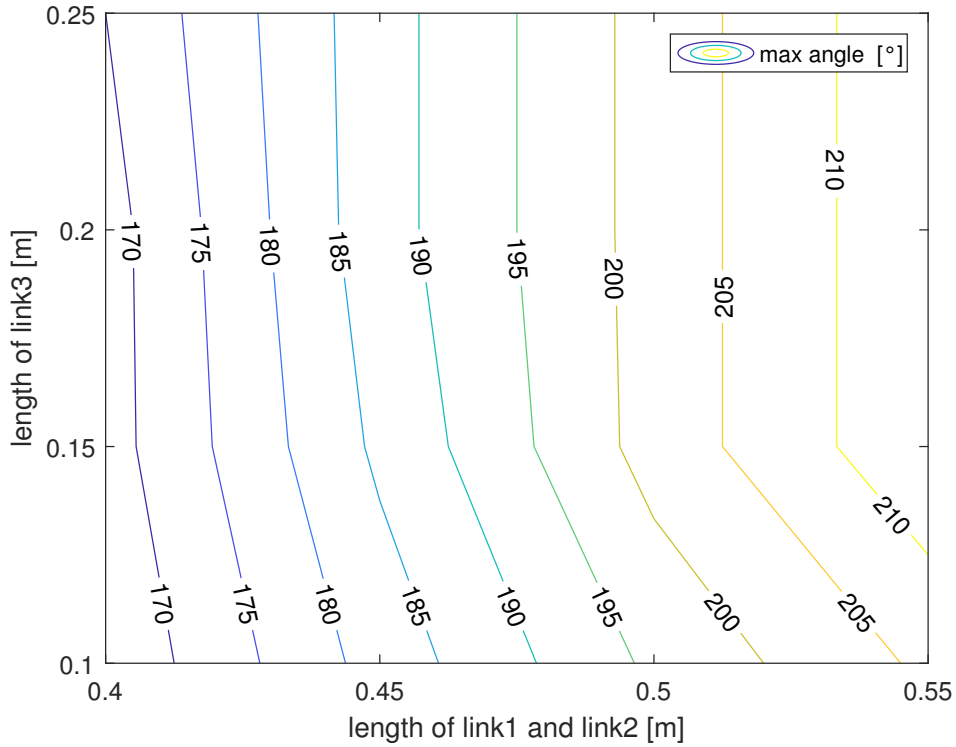
Figure 5.6: Optimization results for a smaller interval of input link lengths

In the end, we confirmed with CompoTech that the first and second link will be 500 millimeters long, and the third link will be 150 millimeters.

We have made a ROS simulation of the robot arm and found out that it can reach further than the collision checker computed. The robot arm dimensions meet the requirements.

Chapter 6

Trajectory planning software

We discussed with CompoTech how the robot would be used by their employees. We examined the CompoTech production process from a product specification to its manufacturing on an existing machine. We focused on the RAFL system in Figure 3.8.

CompoTech's RAFL system consists of a FANUC robot arm attached to linear rail and separately driven rotation axis. CompoTech cooperated with ARC-Robotics [18] on this machine. Together they have created a control software bundle and communication protocol based on TCP/IP. Input data is a configuration file for a product type that is parsed by a program called Shneg 1.0. Shneg 1.0 translates the parameters and sends data in custom TCP/IP protocol into the robot control unit (Figure 6.1).
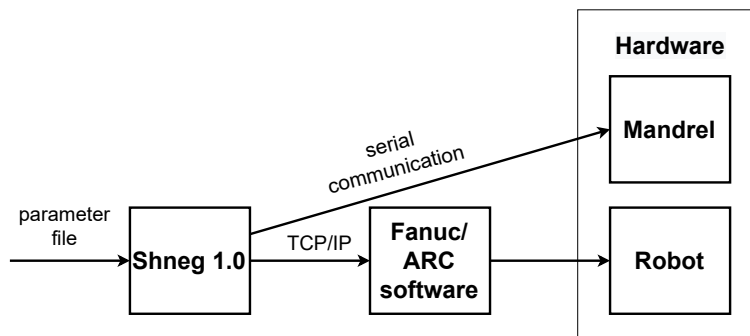
Figure 6.1: Data flow of Compotech RAFL system. From parameter file (left) to the robot (right)

We decided to follow a similar structure, so the input files would be the same as for the existing RAFL system. However, we would not be able to prepare a software bundle for all product types on time, so we chose the ILT tube (Fig. 6.2). It is quite complex, and currently, they are manufactured only on X-winder.
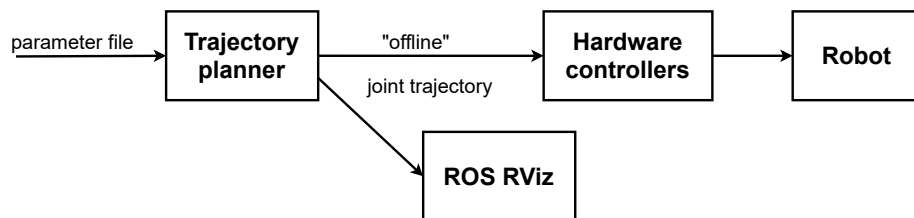
Figure 6.2: ILT tube

Figure 6.3: Data flow of our robot system. From parameter file (left) to the robot (right)

Data flow for our system would be as follows (Figure 6.3). The input file with all necessary parameters would go directly into trajectory planner, which computes all necessary waypoints. The planner then uses ROS and MoveIt planners to generate joint trajectory with time stamps and velocities. The trajectory is then visualized in RViz, so the machine operator can check that the trajectory is correct. Then the trajectory is exported and sent to controllers of physical hardware.

Trajectory planning also presented few issues. Our robot system's structure simplified into a graph does not (Figure 6.4) have a world coordinate system at the beginning. ROS can only work with robotic structures that are open chains, the world coordinate system is situated at one end and end effector or nozzle at the other end. Therefore, we came up with two solutions how to alter our robot's structure.
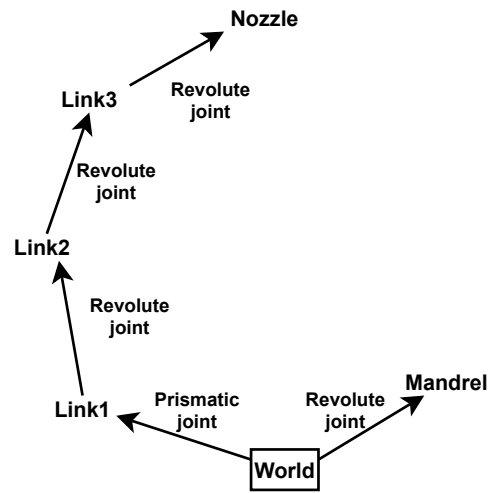
Figure 6.4: Our robot's structure as a graph

The first possible solution is to reorganize where the robot is connected to the world reference coordinate system (Figure 6.5). We could attach the world coordinate system to the rotational mandrel, but visualization would be very confusing since the whole robot system would spin around the mandrel, which would appear stationary.

This solution would also require path constraints or optimization since the requirements only specify the relative position of the nozzle to the mandrel. To explain why, we will use axial fibers as an example. The robot arm can cover 220 degrees around the mandrel with axial fibers without rotating the mandrel. This was simulated in Chapter 5. The robot can also cover the mandrel in axial fibers by only rotating the mandrel and moving the carriage. There are several solutions to this task. We would need to specify path constraints or optimization function, so we have only one solution to this task.
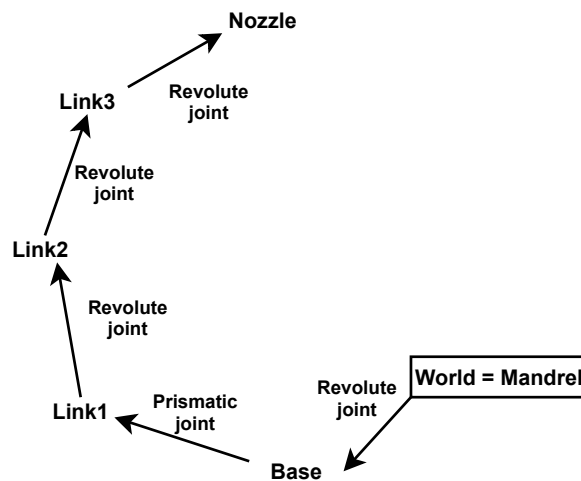
Figure 6.5: First solution on how to define our robot as open chain

The second possible solution is to divide the robot into two separate planning groups (Figure 6.6). One group being the robot arm and the other being the mandrel rotation. This corresponds to CompoTech's RAFL system, and their engineers do use a number of mandrel revolutions as a parameter in their parameter file.
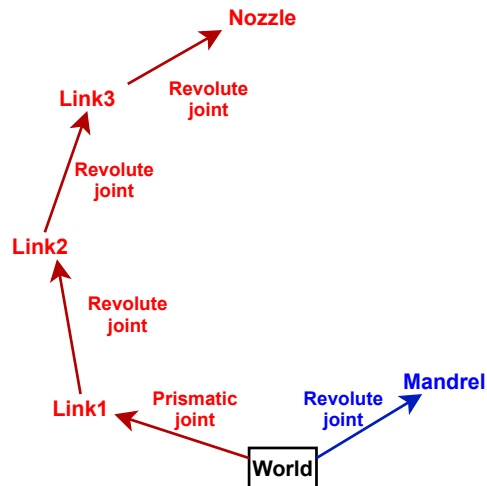
Figure 6.6: Second solution on how to define our robot as open chain, the red part represents arm planning group and the blue part mandrel planning group

We selected the second solution. To generate two separate trajectories and synchronize them was not a problem, but to visualize them synchronously in RViz is not possible with versions of ROS and MoveIt we have used. We also wrote our code in Python which is not as supported by ROS as C++.

■ 6.1   The input of the trajectory planner

The input of the trajectory planner is a `.ldat` file with parameters. This parameter file looks as follows:

```
// ### Definition of product's geometry ###

POJ_nulova = 150;                        // [mm]
vzdalenost_oka = 500;        // [mm]
prumer_trnu_valcova_cast = 30;   // [mm]
oko1_trn_prumer = 40;                // [mm]
oko2_trn_prumer = 40;                // [mm]
trn_prurez = 15;                     // [mm]
uhel_oko1vs2 = 90;                   // [degree]


// ### Definition of manufacturing ###

pocet_cyklu = 22;                    // [1]
pocet_vzoru = 1;                     // [1]
otoc_valcova_cast = 1;               // [otacky]
rychlost_navijeni = 100;             // [%]
typ_ovijeni_oko1 = 0;                // [1] 0=xxx, 1=ss, 2=ddd
typ_ovijeni_oko2 = 0;                // [1] 0=xxx, 1=ss, 2=ddd

okolo_cepu_offset = 10;              // [mm]
vzdalenost_od_osy = 20;              // [mm]
```
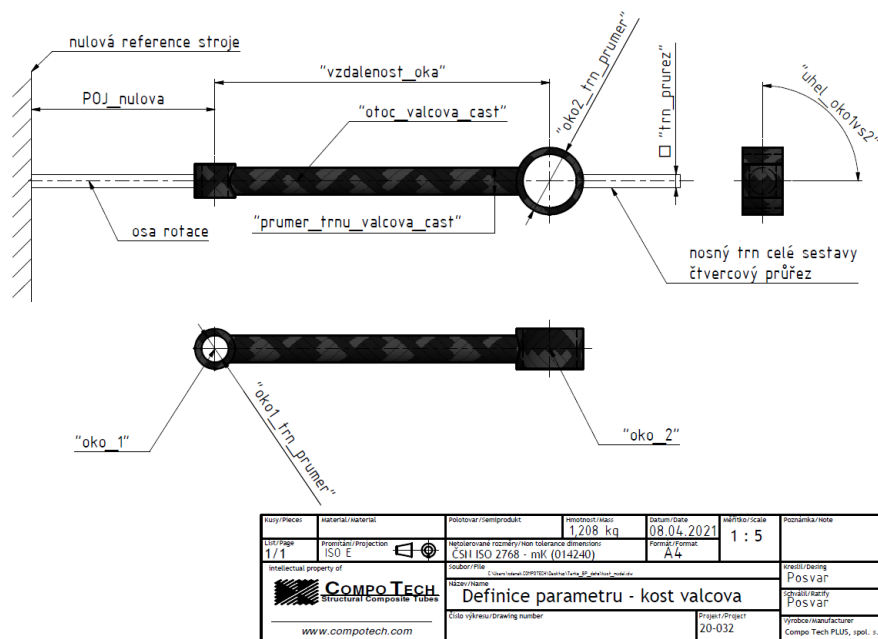
The first part of the parameter file contains variables that describe product's geometry (Fig. 6.7). `POJ_nulova` represents a distance from zero position of the machine to the first loop in millimeters. `vzdalenost_oka` is a distance between end loops in millimeters. `prumer_trnu_valcova_cast` is a diameter of the tube part. `oko1_trn_prumer` and `oko2_trn_prumer` represent diameters of the first and second loop respectively. `trn_prurez` is a diameter of circumscribed circle around a part of mandrel that carries the main part (the part that will be layered with carbon fiber). `uhel_oko1vs2` is an angle between the loops.

Figure 6.7: Schematic of the ILT tube with marked parameters. Provided by CompoTech.

The second part of the parameter file contains variables that define a pattern of laid fiber. `pocet_cyklu` is a number of a cycles. One cycle is when the fiber is laid from one end of mandrel to the other and back. One cycle consists of two runs, which means that the carriage runs from one end of mandrel to the other end. `pocet_vzoru` is a number of patterns on the tube circumference. A pattern is shown in Figure 6.8. `otoc_valcova_cast` is a number of mandrel revolutions per the carriage run. `rychlost_navijeni` is a speed of the machine as a percentage of maximum speed.

35
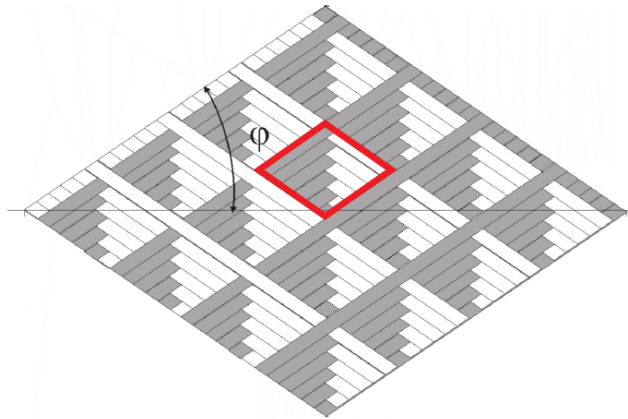
Figure 6.8: A schematic example of a diamond pattern that is created when fibers are wound. The red shape marks one pattern. Provided by CompoTech.

`typ_ovijeni_oko1` and `typ_ovijeni_oko2` represents how are the end loops supposed to be wound. There are two basic techniques and the third one is a combination of the previous two.

The technique marked with '1' is called part loop. The part loop technique means that the loop is wrapped around the loop without the fiber crossing over itself. The trajectory of the part loop technique is shown in Figure 6.9.
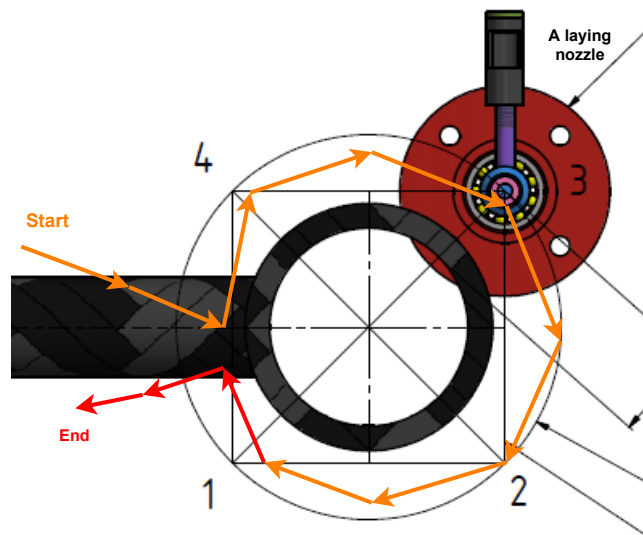
Figure 6.9: Orange and red arrows represent the nozzle trajectory of the part loop technique. The red circle is the nozzle. Provided by CompoTech.

The technique marked with '2' is called full loop. The full loop technique means that the loop is wrapped with the fiber crossing over itself and wrapping all around. The trajectory of the full loop technique is shown in Figure 6.9.
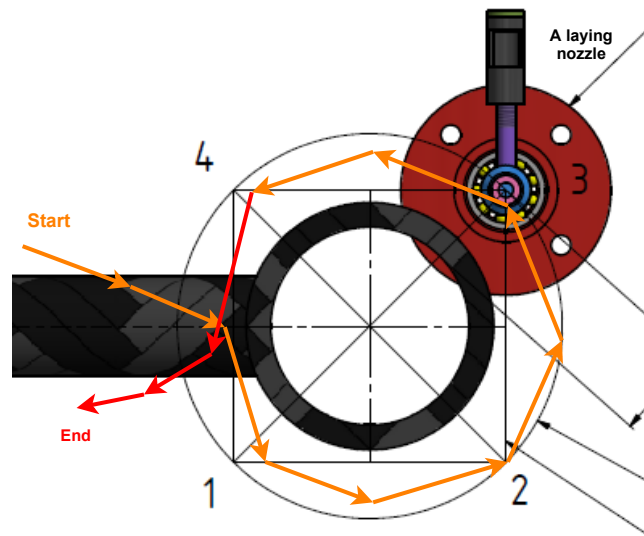
Figure 6.10: Orange and red arrows represent the nozzle trajectory of the full loop technique. The red circle is the nozzle. Provided by CompoTech.

The technique marked '0' is a combination of part loop and full loop. If the nozzle is closer to the point 4 in Figure 6.10 (or 6.9) after it finished one run (carriage translation from one end of the mandrel to the other and mandrel rotation), then the part loop technique is executed. If the nozzle is closer to the point 1 in Figure 6.10 (or 6.9) after it finished one run, then the full loop technique is executed.

The parameter `okolo_cepu_offset` represents an offset of the nozzle from the end loops, so the nozzle will not collide with the mandrel. `vzdalenost_od_osy` is an offset of the nozzle from the tubular part of the mandrel.

■ 6.2 The output of the trajectory planner

The final trajectory is saved as a sequence of points in joint coordinates
with velocities, accelerations and time stamps. The structure corresponds to
`JointTrajectory` ROS message, and it is as follows:

```
Header  header
        uint32  seq
        time  stamp
        string  frame_id
string[]  joint_names
JointTrajectoryPoint[]  points
        float64[]  positions
        float64[]  velocities
        float64[]  accelerations
        float64[]  effort
        duration  time_from_start
```

The header contains `seq`, `time stamp` and `frame_id`. ID sequence `seq` is
left empty since it is irrelevant to our use. `frame_id` is a name of a planning
group.

`joint_names` is an array with joint names. The order of joints in this array
is respected by `JointTrajectoryPoint points` points.

`JointTrajectoryPoint points` is an array of points which are defined
with `positions` array, `velocities` array, `accelerations` array, `effort` array
and `time_from_start`. `positions` are joint coordinates. `effort` is always
empty since our planning and simulation does not consider physical forces.

Every element in `JointTrajectoryPoint points` represent one point in
the trajectory. The whole trajectory is contained in this array.

The format can be altered to correspond with hardware controllers' require-
ments.

Chapter 7

Conclusion

In this thesis, we designed a robot for carbon fiber laying. This robot is based on X-Winder winding machine with an added planar robotic arm with three degrees of freedom.

We created the robot model in ROS, simulated and visualized it in RViz. We wrote a program that checks if required robot positions are possible and if there are no collisions for given lengths of robot links. The program has been used to optimize the robot arm's dimensions.

We have also researched problem with detecting pins and avoiding collisions with them. We have decided to mount a laser triangulation displacement sensor Micro-Epsilon optoNCDT ILD420-200 onto robot arm. The pins would be scanned before actual production, and their positions saved. This process has been simulated with a variety of pins attached to the turntable and detecting them with the sensor. In conclusion, the sensor optoNCDT measures the pin's real position reliably.

Then we wrote a trajectory planning software that generates collision-free trajectory based on input parameter file. We encountered a problem with our robot structure which is not supported by ROS. We decided to divide the machine into two planning groups, the robot arm and the rotating mandrel, and synchronize those trajectories in time.

The operation personnel provides parameters of the ILT tube as an input (length of the tube, the diameter of the tube and both end loops, number of cycles, etc.). The planner will generate a trajectory for the winding process and visualize it, so the personnel can check and confirm that the trajectory is correct. Then the trajectory is saved as a sequence of joint coordinates, velocities, accelerations and time stamps, so the hardware controllers can execute the trajectory.

During the upcoming summer, we will continue to work with CompoTech to build a proposed robot for carbon fiber laying.

Bibliography

[1]   *CompoTech Plus s. r. o.* 2021. URL: https://compotech.com/.

[2]   Stan Peters. *Composite Filament Winding.* 2011.

[3]   Ondřej Uher. *Axial fibre filament winding: A technique full of promise.* Jan. 2003.

[4]   *Keeping joint design in the loop.* URL: https://www.composites.media/keeping-joint-design-in-the-loop/.

[5]   Jeff Sloan. *The first composite fuselage section for the first composite commercial jet.* 2018. URL: https://www.compositesworld.com/articles/the-first-composite-fuselage-section-for-the-first-composite-commercial-jet.

[6]   *Automated Dynamics.* 2021. URL: http://www.automateddynamics.com/composite-structures.

[7]   *Autoclave example.* 2021. URL: https://www.compositesone.com/process/autoclave/.

[8]   *SGL develops pre-impregnated towpregs.* 2015. URL: https://www.materialstoday.com/composite-processing/news/sgl-develops-pre-impregnated-towpregs/.

[9]   *Automated Fiber Placement.* 2012. URL: https://mikrosam.com/new/article/en/automated-fiber-placement-the-complete-system/.

[10]   *Suppliers for Automated fiber placement machines.* 2021. URL: https://www.compositesworld.com/suppliers/product/245.

[11]   *Ingersoll Machine Tools, Inc.* 2021. URL: https://en.machinetools.camozzi.com/products/composite-manufacturing/all-products/mongoose.kl.

[12]   Dale Brosius. *Out-of-autoclave manufacturing: The green solution.* 2014. URL: https://www.compositesworld.com/articles/out-of-autoclave-manufacturing-the-green-solution.

[13]   *Automated systems MF TECH.* 2021. URL: https://mftech.fr/en/process-2/.

[14]   *X-winder, The Original Desktop Filament Winder.* 2021. URL: https://xwinder.com/.

[15] *MICRO-EPSILON Czech Republic.* 2021. URL: https://www.micro-epsilon.cz/.

[16] *The Robot Operating System (ROS).* 2021. URL: https://www.ros.org/.

[17] *MoveIt Motion Planning Framework.* 2021. URL: https://moveit.ros.org/.

[18] *ARC-Robotics s.r.o.* 2021. URL: https://www.arc-robotics.cz/.